Communications in Nonlinear Science and Numerical Simulation 126 (2023) 107432

Contents lists available at ScienceDirect

Communications in Nonlinear Science and Numerical Simulation

journal homepage: www.elsevier.com/locate/cnsns

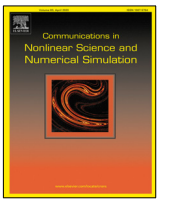

Research paper

# Fractional forward Kolmogorov equations in population genetics

Somayeh Mashayekhi

*Department of Mathematics, Kennesaw State University, Marietta, GA 30060, United States of America*

ARTICLE INFO

*Article history:*
Received 27 February 2023
Received in revised form 4 June 2023
Accepted 10 July 2023
Available online 17 July 2023

*Keywords:*
Population genetics
Heterogeneity
Fractional forward Kolmogorov equations
Least squares approximation
Numerical solution

ABSTRACT

This paper combines theoretical development and numerical methods to characterize the effect of heterogeneity in population genetics. To address heterogeneity in population genetics, we build the first fractional forward Kolmogorov equations in population genetics, where the distribution of the allele frequencies of a given set of loci in a population is a solution of forward Kolmogorov equations. This framework will be implemented, and the model will be studied computationally. To study the model, a new numerical method for solving the fractional partial differential equations is presented. The method is based upon the least squares approximation via Legendre polynomials. The Riemann–Liouville fractional integral operator for Legendre polynomials is utilized to reduce the solution of the fractional partial differential equations to a system of algebraic equations. The error bound and the stability of the method are presented. Illustrative examples are included to demonstrate the validity and applicability of the technique. Using the new numerical method, we derive the allele frequency distribution as a solution of the fractional forward Kolmogorov equations. We study the behavior of allele frequency distribution by considering the effect of evolutionary and demographic forces. This study shows that heterogeneity changes the behavior of the distribution of the allele frequencies.



## 1. Introduction

A central goal of population genetics is to infer the history of populations and describe the evolutionary forces that have shaped their genetic variation [1]. The benefit of this field includes the studies of human history, which aim to map the genes that cause human disease [2]. To study the evolutionary history of a population, we need an explicit model that presents the effect of evolutionary and demographic forces such as genetic drift, mutation, selection, and immigration. The Wright–Fisher model [3,4] and Kingman coalescent model [5–8] occupy an important role in this area. The coalescent process is dual to the Wright–Fisher model.

The Wright–Fisher model, which describes the evolution of a population forward in time, is a mathematical framework for modeling allele frequency data. Although the dynamics of the Wright–Fisher model are well understood, a simple closed-form analytical expression for the distribution of allele frequencies (DAF) is unknown [1]. The diffusion approximation is a well-known method for calculating the DAF by considering the effect of evolutionary and demographic forces [1,9–11].

Although natural populations live in heterogeneous environments, and individuals in these populations have different chances to produce offspring, the current population genetics models assume environmental homogeneity within a

*E-mail addresses:* smashayekhi@fsu.edu, smashay1@kennesaw.edu.

https://doi.org/10.1016/j.cnsns.2023.107432
1007-5704/

population. There is a critical need to develop the study of the effects of a heterogeneous environment on offspring production. For example, the impact of heterogeneity on tumor cells and its effect on the distribution of allele frequencies (DAF) is an open and challenging question. The answer to this question provides the novel insight needed to confront the problem of therapeutic resistance in tumors [12–14]. There is a distinct lack of theory and tools available to investigate the impact of heterogeneity. Recently, Mashayekhi et al. have introduced a framework that includes the effect of heterogeneity [15]. Their work is based on generalizing the coalescent process using a recent advancement in fractional calculus called the fractional coalescent or $f$-coalescent. Because the coalescent is typically restricted to a handful of individuals and does not use allele frequency data, in this paper, we introduce a new theory that will focus on the effect of heterogeneity by applying fractional calculus to infer the distribution of allele frequencies (DAF). Because the closed analytical form of an allele frequency distribution (DAF) as a function of time is not available, our approximations will be built on the diffusion limit.

Fractional calculus has a long history in mathematics, dating back to integer order calculus, but it gained traction recently. In recent years, it has been shown that fractional calculus can capture physical and biological phenomena better than integer-order calculus and is a powerful tool to detect potential environmental heterogeneity within a population [15–22]. Another recent example is the work of [23], who used fractional-order derivatives to model the properties of the SARS CoV-2 protease.

To study the effect of heterogeneity, we introduce the fractional forward Kolmogorov equations in population genetics. The DAF at any time is the solution of fractional forward Kolmogorov equations. We use the fractional Taylor series [24] to derive this equation. The infinitesimal mean and variance are important factors defining the forward Kolmogorov equations in population genetics.

Developing the computational methods for solving the diffusion equations arising in population genetics has been considered in the literature (for more details, please see [1]). Since the fractional partial differential equations (FPDEs) have shown to be adequate models for various physical phenomena [25], Finding reliable and robust numerical and analytical methods for solving FPDEs has been focused on in the last two decades [26]. Recently, several numerical methods to solve FPDEs have been given, such as the Laplace transform method [27], generalized differential transform method [28], the Fourier technique [29], Adomiande composition method (ADM) [30], He's homotopy perturbation method (HPM) [31], homotopy analysis method (HAM) [32] and Kansa method [33].

To study the behavior of fractional forward Kolmogorov equations in population genetics, we introduce an effective computational method to solve FPDEs. The method is based upon the least squares approximation via Legendre polynomials. We first convert FPDEs to an equivalent system of differential equations by using Legendre pseudo-spectral discretization method. The Riemann–Liouville fractional integral operator for Legendre polynomials is then utilized to reduce the solution of the system of differential equations to the solution of algebraic equations. We study the error bound and the stability of the new method and solve some numerical examples to demonstrate the validity and applicability of the technique. We use the new numerical method to derive the allele frequency distribution as a solution for the fractional forward Kolmogorov equations in population genetics. We study the DAF by considering the effect of evolutionary and demographic forces such as genetic drift and mutation. This study shows that heterogeneity changes the behavior of the distribution of the allele frequencies.

The outline of this paper is as follows: In Section 2, we introduce some necessary definitions and mathematical preliminaries of fractional calculus. Section 3 presents the fractional forward Kolmogorov equations in population genetics. Section 4 is devoted to the numerical method for solving FPDEs. In Section 5, We study the DAF by considering the effect of evolutionary and demographic forces using the new numerical method.

## 2. Preliminaries and notations

There are various definitions of fractional derivative and integration. The widely used definition of a fractional derivative is the Caputo definition, and a fractional integration is a Riemann–Liouville definition. We consider the Caputo form because it has been shown that in applied problems, this derivative works more effectively than others [16]. The fractional derivative is denoted by $D_t^\alpha$, where $\alpha$ is the fractional order with respect to $t$. For a function $u(x,t)$, the Caputo form of the fractional derivative with respect to $t$ is [34]

$$D_t^\alpha u(x,t) = \frac{\partial^\alpha u(x,t)}{\partial t^\alpha} = \frac{1}{\Gamma(n-\alpha)} \int_0^t \frac{\frac{\partial^n u(x,s)}{\partial s^n}}{(t-s)^{\alpha+1-n}} ds, \quad (n-1) < \alpha \le n, \ n \in \mathbb{N}, \tag{1}$$

where $\alpha > 0$ is the order of the derivative and $n$ is the smallest integer greater than $\alpha$. The Riemann–Liouville fractional integral operator of order $\alpha$ with respect to $t$ is defined as [27]

$$I^\alpha u(x,t) = \begin{cases} \frac{1}{\Gamma(\alpha)} \int_0^t \frac{u(x,s)}{(t-s)^{1-\alpha}} ds = \frac{1}{\Gamma(\alpha)} t^{\alpha-1} * u(x,t), & \alpha > 0, \\ u(x,t), & \alpha = 0. \end{cases} \tag{2}$$

where $t^{\alpha-1} * u(x,t)$ is the convolution product of $t^{\alpha-1}$ and $u(x,t)$ with respect to $t$. The Caputo derivative and Riemann–Liouville integral satisfy the following property [27]

$$I^\alpha (D_t^\alpha u(x,t)) = u(x,t) - \sum_{k=0}^{n-1} u^k(x,0) \frac{t^k}{k!}. \tag{3}$$

## 3. Fractional forward Kolmogorov equations in population genetics

In this section, we introduce the fractional forward Kolmogorov equations in population genetics, where the distribution of allele frequencies (DAF) is the solution of this equation. To introduce the fractional forward Kolmogorov equations, we use the properties of fractional calculus, specifically, the fractional Taylor series. A fractional power series expansion is obtained for different definitions of the fractional derivative as a generalization of the Taylor power series [35]. The fractional Taylor series in the Caputo form has been introduced in [36]. Let us assume $u(x, t)$ is the distribution of allele frequency, a function of allele frequency, $x$, and time, $t$. Assuming the Chapman–Kolmogorov (CK) equation in terms of probabilities has the following form

$$u(x, t+\delta t) = \int P(x, x')u(x', t)dx', \tag{4}$$

Eq. (4) states that the present allele frequency distribution is obtained by integrating all prior histories. Let us assume the transition occurs in a short time $\delta t$, and the change is by a small amount $\delta x = x - x'$. Using the fractional Taylor series with respect to $t$, we have

$$u(x, t+\delta t) = u(x, t) + \frac{(\delta t)^\alpha}{\Gamma(\alpha+1)} D_t^\alpha u(x, t) + \cdots \tag{5}$$

Using Eqs. (4) and (5) and Taylor series of $P(x-\delta x, \delta x)$ and $u(x-\delta x, t)$ with respect to $x$ we have [37]

$$\begin{aligned}&\frac{1}{\Gamma(\alpha+1)} D_t^\alpha u(x, t) + \cdots \approx -(u(x, t)\frac{\partial a(x)}{\partial x} + a(x)\frac{\partial u(x, t)}{\partial x}) + \\ &\frac{1}{2}(u(x, t)\frac{\partial^2 b(x)}{\partial x^2} + 2\frac{\partial u(x, t)}{\partial x}\frac{\partial b(x)}{\partial x} + b(x)\frac{\partial^2 u(x, t)}{\partial x^2}) + \cdots,\end{aligned} \tag{6}$$

where

$$\frac{1}{(\delta t)^\alpha}\int P(x, \delta x)(\delta x)d(\delta x) = a(x), \tag{7}$$

$$\frac{1}{(\delta t)^\alpha}\int P(x, \delta x)(\delta x)^2 d(\delta x) = b(x). \tag{8}$$

where we define a new time scale by $(\delta t)^\alpha = \frac{1}{2N}$ such that one-time unit to the $\alpha$ corresponds to $2N$ generations. Using Eqs. (6)–(8) we have

$$D_t^\alpha u(x, t) = -\Gamma(\alpha+1)\frac{\partial(a(x)u(x, t))}{\partial x} + \frac{\Gamma(\alpha+1)}{2}\frac{\partial^2(b(x)u(x, t))}{\partial x^2}. \tag{9}$$

where $a(x)$ and $b(x)$ have different forms depending on the evolutionary forces. Since the coalescent process and the forward process are inverse processes [38–40], the order of fractional derivatives in Eq. (9) is the candidate to show the effect of heterogeneity in the population [15]. In the next section, we introduce the new numerical method for solving the general form of the fractional partial differential equations to study the properties of Eq. (9).

## 4. Fractional partial differential equations

In this section, we develop a new numerical method for the general form of the fractional partial differential equation (FPDE) as

$$\begin{cases} \gamma_1(x)\frac{\partial^\alpha u(x,t)}{\partial t^\alpha} + \gamma_2(x)\frac{\partial^{\alpha-1} u(x,t)}{\partial t^{\alpha-1}} + \gamma_3(x)u(x, t) + \gamma_4(x)\frac{\partial u(x,t)}{\partial x} + \gamma_5(x)\frac{\partial^2 u(x,t)}{\partial x^2} = f(x, t), \\ u(0, t) = h_1(t), \quad u(L, t) = h_2(t), \quad 0 < t < 1, \\ u(x, 0) = g_1(x), \quad u_t(x, 0) = g_2(x), \quad 0 \le x \le L \end{cases} \tag{10}$$

where $1 < \alpha \le 2$. Eq. (9) is a specific form of Eq. (10) where we assume $\gamma_1(x) = 0$. We use least-squares approximation via Legendre polynomials to introduce the new numerical method for solving Eq. (10). Suppose $\Psi(t)$ and a vector of base functions

$$G(t) = [L_0(t),\ L_1(t), \ldots, L_M(t)]^T$$

are defined on $t \in (-1, 1)$ where

$$L_m(t) = \sum_{k=0}^{m} \binom{m}{k}\binom{m}{m-k}(\frac{t-1}{2})^k(\frac{t+1}{2})^{m-k}, \tag{11}$$

and

$$\binom{z}{n} = \begin{cases} \frac{\Gamma(z+1)}{\Gamma(n+1)\Gamma(z-n+1)}, & n \geq 0, \\ 0, & n < 0. \end{cases} \tag{12}$$

For the least squares approximation, the coefficients $c_0,\ c_1, \ldots, c_M$ of the sum [41]

$$\Psi_M^G(t) = c_0 L_0(t) + c_1 L_1(t) + \cdots + c_M L_M(t), \tag{13}$$

must be determined in such a way that the integral

$$I_M^G = \int_{-1}^{1} (\Psi(t) - \Psi_M^G(t))^2 dt, \tag{14}$$

is minimal. The function $\Psi_M^G(t)$ with these coefficients is the least squares fit of $\Psi(t)$ concerning vector $G$. The piecewise least-squares approximation is a powerful method to increase the accuracy of the approximation [42]. This method divides the original interval $(-1, 1)$ into several smaller sectors and defines each sector's local sets $L_m(t)$. For details concerning this procedure, see [41,43].

It is easy to show, by using the properties of Legendre polynomials and fractional integral, we have

$$I^{\alpha}(L_m(t)) = 2^m \sum_{k=0}^{m} \binom{m}{k} \binom{\frac{m+k-1}{2}}{m} \frac{\Gamma(k+1)}{\Gamma(k+1+\alpha)} t^{k+\alpha}. \tag{15}$$

### *4.1. Legendre pseudo-spectral spatial discretization for FPDEs*

In this section, we apply pseudo-spectral spatial discretization based on Legendre–Gauss–Lobatto collocation points to convert Eq. (10) to an equivalent system of linear ordinary differential equations. The Legendre–Gauss–Lobatto collocation points are the roots of $L_{K+1}(x) - L_{K-1}(x)$ where $L_{K+1}(x)$ and $L_{K-1}(x)$ are the Legendre polynomials of the order $K+1$ and $K-1$. Since these points include $-1$ and 1, they are the best choice for discretization if $-1$ and 1 are the bounds of the domain. To use Legendre–Gauss–Lobatto points $w_i$ for discrediting Eq. (10), we first transform $w_i \in [-1, 1]$ to $x_i, y_i \in [0, L]$ by using the following transformation

$$x_i = y_i = \frac{L}{2} w_i + \frac{L}{2}, \qquad i = 0, 1, \ldots, K. \tag{16}$$

By substituting $x_i$ given in Eq. (16) in Eq. (10), for $i = 1, \ldots, K-1$, we have

$$\gamma_1(x_i) \frac{\partial^{\alpha} u(x_i, t)}{\partial t^{\alpha}} + \gamma_2(x_i) \frac{\partial^{\alpha-1} u(x_i, t)}{\partial t^{\alpha-1}} + \gamma_3(x_i) u(x_i, t) + \gamma_4(x_i) \sum_{j=1}^{K-1} d_{ij}^1 u(x_j, t) + \gamma_5(x_i) \sum_{j=1}^{K-1} d_{ij}^2 u(x_j, t) = h(x_i, t), \ t > 0 \tag{17}$$

where $u(x_i, 0) = g_1(x_i)$, $u_t(x_i, 0) = g_2(x_i)$, $i = 1, \ldots, K-1$, and $x_i$ is Legendre–Gauss–Lobatto collocation point and $h(x_i, t)$ is given by

$$h(x_i, t) = f(x_i, t) - \gamma_4(x_i)(d_{i0}^1 h_1(t) + d_{iK}^1 h_2(t)) - \gamma_5(x_i)(d_{i0}^2 h_1(t) + d_{iK}^2 h_2(t)),$$

and, $d_{ij}^1$ and $d_{ij}^2$ are the elements of the differential matrices which are introduced in [44] as

$$d_{ij}^1 = \begin{cases} \frac{L_{K-1}(x_i)}{L_{K-1}(x_j)} \cdot \frac{1}{x_i - x_j} & i \neq j \\ -\frac{(K-1)K}{4} & i = j = 0 \\ \frac{(K+1)K}{4} & i = j = K-1 \\ 0 & \text{otherwise} \end{cases}$$

and

$$d_{ij}^2 = \begin{cases} -2\frac{L_{K-1}(x_i)}{L_{K-1}(x_j)} \cdot \frac{1}{(x_i - x_j)^2} & 1 \leq i \leq K-2, \quad 0 \leq j \leq K-1, \quad i \neq j, \\ \frac{L''(x_j)}{3L_{K-1}(x_j)}, & 1 \leq i = j = \leq K-2 \\ \frac{(-1)^{K-1}}{L_{K-1}(x_j)} \frac{(K-1)K(1+x_j)-4}{2(1+x_j)^2}, & i = 0, \quad 1 \leq j \leq K-1, \\ \frac{1}{L_{K-1}(x_j)} \frac{(K-1)K(1-x_j)-4}{2(1-x_j)^2}, & i = K-1, \quad 0 \leq j \leq K-2, \\ \frac{(K-1)K(K^2-K-2)}{24}, & i = j = 0, \quad i = j = K-1 \end{cases}$$

where $L_K$ is a Legendre polynomial of order $K$. The system in Eq. (17) can be rewritten as

$$\gamma_1^* \frac{\partial^\alpha U^1(t)}{\partial t^\alpha} + \gamma_2^* \frac{\partial^{\alpha-1} U^1(t)}{\partial t^{\alpha-1}} + \gamma_3^* U^1(t) + \gamma_4^* D^1 U^1(t) + \gamma_5^* D^2 U^1(t) = W^1(t), \tag{18}$$

where

$$U^1(t) = [u(x_1, t), u(x_2, t), \ldots, u(x_{K-1}, t)]^T,$$

$$W^1(t) = [h(x_1 t), h(x_2, t), \ldots, h(x_{K-1}, t)]^T,$$

$$\gamma_i^* = \begin{bmatrix} \gamma_i(x_1) & 0 & 0 & \ldots & 0 \\ 0 & \gamma_i(x_2) & 0 & \ldots & 0 \\ \vdots & & & & \\ 0 & 0 & 0 & \ldots & \gamma_i(x_{K-1}) \end{bmatrix},$$

and $D^1 = [d_{ij}^1]$ and $D^2 = [d_{ij}^2]$ are derivative matrices of order $(K-1) \times (K-1)$. By this discretization, we will solve the system in Eq. (18) rather than those given by Eq. (10).

### 4.2. Numerical method

This section uses the least-squares approximation via Legendre polynomials for solving Eq. (18). Le's assume $m = 0, 1, \ldots, M$ is the order of Legendre polynomials. First, using Eq. (13), we expand $\frac{\partial^\alpha u(x_i,t)}{\partial t^\alpha}$ as

$$\frac{\partial^\alpha u(x_i, t)}{\partial t^\alpha} = A_i^T \overline{G}(t), \qquad i = 1, \ldots, K-1, \tag{19}$$

where

$$A_i^T = [a_0^i, a_1^i, \ldots, a_M^i], \qquad i = 1, \ldots, K-1, \qquad \overline{G}(t) = [L_0(2t-1),\ L_1(2t-1), \ldots, L_M(2t-1)]^T. \tag{20}$$

Using Eqs. (3) and (19), we obtain

$$u(x_i, t) = A_i^T \overline{G}(t, \alpha) + g_2(x_i)t + g_1(x_i) \qquad i = 1, \ldots, K-1, \tag{21}$$

$$\frac{\partial^{\alpha-1} u(x_i, t)}{\partial t^{\alpha-1}} = A_i^T \overline{G}(t, 1) + \frac{g_2(x_i)}{\Gamma(3-\alpha)} t^{2-\alpha}, \qquad i = 1, \ldots, K-1, \tag{22}$$

where

$$\overline{G}(t, \alpha) = [I^\alpha(L_0(2t-1)), I^\alpha(L_1(2t-1)), \ldots, I^\alpha(L_M(2t-1))]^T,$$

$$\overline{G}(t, 1) = [I^1(L_0(2t-1)), I^1(L_1(2t-1)), \ldots, I^1(L_M(2t-1))]^T.$$

Using Eq. (19) we have

$$\frac{\partial^\alpha U^1(t)}{\partial t^\alpha} = [A_1^T \overline{G}(t), A_2^T \overline{G}(t), \ldots, A_{K-1}^T \overline{G}(t)]^T = \mathbb{A}^T \widehat{G_1(t)}, \tag{23}$$

and from Eqs. (19)–(22), we have

$$U^1(t) = [A_1^T \overline{G}(t, \alpha) + g_2(x_1)t + g_1(x_1), \ldots, A_{K-1}^T \overline{G}(t, \alpha) + g_2(x_{K-1})t + g_1(x_{K-1})]^T = \mathbb{A}^T \widehat{G_1(t, \alpha)} + \widehat{\phi_1}, \tag{24}$$

$$\frac{\partial^{\alpha-1} U^1(t)}{\partial t^{\alpha-1}} = [A_1^T \overline{G}(t, 1) + \frac{g_2(x_1)}{\Gamma(3-\alpha)} t^{2-\alpha} + \cdots + A_{K-1}^T \overline{G}(t, 1) + \frac{g_2(x_{K-1})}{\Gamma(3-\alpha)} t^{2-\alpha}]^T = \mathbb{A}^T \widehat{G_1(t, 1)} + \widehat{\phi_2}, \tag{25}$$

where

$$\mathbb{A}^T = \begin{bmatrix} A_1^T \\ A_2^T \\ \vdots \\ A_{K-1}^T \end{bmatrix} = \begin{bmatrix} a_0^1 & a_1^1 & \ldots & a_M^1 \\ a_0^2 & a_1^2 & \ldots & a_M^2 \\ \vdots & & & \\ a_0^{K-1} & a_1^{K-1} & \ldots & a_M^{K-1} \end{bmatrix},$$

and

$$\widehat{\phi_1} = [g_2(x_1)t + g_1(x_1), g_2(x_2)t + g_1(x_2), \ldots, g_2(x_{K-1})t + g_1(x_{K-1})]^T,$$

$$\widehat{\phi_2} = [\frac{g_2(x_1)}{\Gamma(3-\alpha)}t^{2-\alpha}, \frac{g_2(x_2)}{\Gamma(3-\alpha)}t^{2-\alpha}, \ldots, \frac{g_2(x_{K-1})}{\Gamma(3-\alpha)}t^{2-\alpha}]^T,$$

$$\widehat{G_1(t)} = [\overline{G}(t), \overline{G}(t), \ldots, \overline{G}(t)],$$

$$\widehat{G_1(t,\alpha)} = [\overline{G}(t,\alpha), \overline{G}(t,\alpha), \ldots, \overline{G}(t,\alpha)],$$

$$\widehat{G_1(t,1)} = [\overline{G}(t,1), \overline{G}(t,1), \ldots, \overline{G}(t,1)].$$

Substituting Eqs. (23)–(25) in Eq. (18) we get

$$\gamma_1^* \mathbb{A}^T \widehat{G_1(t)} + \gamma_2^*(\mathbb{A}^T \widehat{G_1(t,1)} + \widehat{\phi_2}) + (\gamma_3^* + \gamma_4^* D^1 + \gamma_5^* D^2)(\mathbb{A}^T \widehat{G_1(t,\alpha)} + \widehat{\phi_1}) = W^1(t), \quad t > 0. \tag{26}$$

We use the collocation method by requiring the residual of the problem, i.e.,

$$\gamma_1^* \mathbb{A}^T \widehat{G_1(t)} + \gamma_2^*(\mathbb{A}^T \widehat{G_1(t,1)} + \widehat{\phi_2}) + (\gamma_3^* + \gamma_4^* D^1 + \gamma_5^* D^2)(\mathbb{A}^T \widehat{G_1(t,\alpha)} + \widehat{\phi_1}) - W^1(t) = 0, \tag{27}$$

to vanish on the collocation points leads to a system of linear algebraic equations which can be solved for the unknown vector $\mathbb{A}^T$. We use Newton–Cotes nodes $t_r$ given by [44]

$$t_r = \frac{r}{M}, \quad r = 0, 1, \ldots, M. \tag{28}$$

as the collocation points.

**Remark 1.** To summarize the numerical method presented in Section 4, we introduce the following algorithm. Let us assume we want to solve the fractional partial differential equation (FPDE) in Eq. (10).

- **Step 1:** We apply pseudo-spectral spatial discretization based on Legendre–Gauss–Lobatto collocation points (Eq. (16)) to convert Eq. (10) to an equivalent system of linear ordinary differential equations. After applying discretization, we get Eq. (18).
- **Step 2:** We develop the numerical method based on the least-squares approximation via Legendre polynomials to solve the system presented in Eq. (18).
  - Using Eqs. (23), (24) and (25) we find the approximation of $\frac{\partial^\alpha U^1(t)}{\partial t^\alpha}$, $U^1(t)$ and $\frac{\partial^{\alpha-1} U^1(t)}{\partial t^{\alpha-1}}$.
  - We substitute Eqs. (23)–(25) in Eq. (18) to get Eq. (26).
  - We use the collocation method by requiring the residual of the problem in Eq. (27) to vanish on the collocation points (Eq. (28)) that lead to a system of linear algebraic equations which can be solved for the unknown vector $\mathbb{A}^T$.
- **Step 3:** Using the vector $\mathbb{A}^T$ and Eq. (24), we find the approximation of the solution of Eq. (10) at the discretization points.

In the next section, we derive the error bound of the new numerical method.

### 4.3. Error bounds

In this section, we derive the error bound of using the best approximation to solve the system in Eq. (18).

**Theorem 1.** *Suppose $u(x_i, t) = u_i(t) \in H^\mu(0, 1)$, the error bound is given by*

$$\|E_i\|_{L^2(0,1)} \leq \frac{\|\gamma_1(x)\|_{L_\infty[0,1]} + \|\gamma_2(x)\|_{L_\infty[0,1]}}{\Gamma(3-\alpha)}(cM^{2r-\frac{1}{2}-\mu}\|u_i^{(\mu)}\|_{L^2(0,1)}) +$$

$$\|\gamma_3(x)\|_{L_\infty[0,1]} cM^{-\mu}\|u_i^{(\mu)}\|_{L^2(0,1)} + \sum_{j=0}^{K}(\|\gamma_4(x)d_{ij}^1\|_{L_\infty[0,1]} + \|\gamma_5(x)d_{ij}^2\|_{L_\infty[0,1]})cM^{-\mu}\|u_j^{(\mu)}\|_{L^2(0,1)}, \tag{29}$$

*where $E_i$ denotes the error bound corresponding to the ith equation in the system presented in Eq. (18).*

**Proof.** Using Eq. (13), let assume $u(x_i,t)_M^G = u_i^G(t)$ is the least square approximation of $u(x_i,t) = u_i(t)$. The modified equation for Eq. (17) is as

$$\begin{aligned}\|E_i\|_{L^2(0,1)} = ||&\gamma_1(x_i)\frac{\partial^\alpha u_i^G(t)}{\partial t^\alpha} + \gamma_2(x_i)\frac{\partial^{\alpha-1}u_i^G(t)}{\partial t^{\alpha-1}} + \gamma_3(x_i)u_i^G(t)\\ &+ \gamma_4(x_i)\sum_{j=1}^{K-1} d_{ij}^1 u_j^G(t) + \gamma_5(x_i)\sum_{j=1}^{K-1} d_{ij}^2 u_j^G(t) - h(x_i,t)||_{L^2(0,1)},\end{aligned} \tag{30}$$

Using Eqs. (17) and (30), we have

$$\begin{aligned}\|E_i\|_{L^2(0,1)} = ||&\gamma_1(x_i)\frac{\partial^\alpha u_i^G(t)}{\partial t^\alpha} + \gamma_2(x_i)\frac{\partial^{\alpha-1}u_i^G(t)}{\partial t^{\alpha-1}} + \gamma_3(x_i)u_i^G(t)\\ &+ \gamma_4(x_i)\sum_{j=1}^{K-1} d_{ij}^1 u_j^G(t) + \gamma_5(x_i)\sum_{j=1}^{K-1} d_{ij}^2 u_j^G(t) - (\gamma_1(x_i)\frac{\partial^\alpha u_i(t)}{\partial t^\alpha} + \gamma_2(x_i)\frac{\partial^{\alpha-1}u_i(t)}{\partial t^{\alpha-1}}\\ &+ \gamma_3(x_i)u_i(t) + \gamma_4(x_i)\sum_{j=1}^{K-1} d_{ij}^1 u_j(t) + \gamma_5(x_i)\sum_{j=1}^{K-1} d_{ij}^2 u_j(t))||_{L^2(0,1)}.\end{aligned} \tag{31}$$

Using Eq. (31), we get

$$\begin{aligned}\|E_i\|_{L^2(0,1)} \le &\|\gamma_1(x)\|_{L_{\infty[0,1]}}\|\frac{\partial^\alpha u_i^G(t)}{\partial t^\alpha} - \frac{\partial^\alpha u_i(t)}{\partial t^\alpha}\|_{L^2(0,1)} + \|\gamma_2(x)\|_{L_{\infty[0,1]}}\|\frac{\partial^{\alpha-1}u_i^G(t)}{\partial t^{\alpha-1}} - \frac{\partial^{\alpha-1}u_i(t)}{\partial t^{\alpha-1}}\|_{L^2(0,1)}\\ &+ \|\gamma_3(x)\|_{L_{\infty[0,1]}}\|u_i^G(t) - u_i(t)\|_{L^2(0,1)} + \sum_{j=1}^{K-1}(\|\gamma_4(x)d_{ij}^1\|_{L_{\infty[0,1]}} + \|\gamma_5(x)d_{ij}^2\|_{L_{\infty[0,1]}})\|u_j^G(t) - u_j(t)\|_{L^2(0,1)},\end{aligned} \tag{32}$$

On the other hand, if $n-1 < \alpha \le n$, we have [41]

$$\|u_i(t) - u_i^G(t)\|_{L^2(0,1)} \le cM^{-\mu}\|u_i^{(\mu)}\|_{L^2(0,1)}, \tag{33}$$

and for $r \ge 1$,

$$\|\frac{\partial^\alpha u_i(t)}{\partial t^\alpha} - \frac{\partial^\alpha u_i^G(t)}{\partial t^\alpha}\|_{L^2(0,1)} \le \frac{cM^{2r-\frac{1}{2}-\mu}\|u_i^{(\mu)}\|_{L^2(0,1)}}{\Gamma(n-\alpha+1)}. \tag{34}$$

Using Eqs. (32)–(34), we get Eq. (29).

*4.3.1. Ulam–Hyers stability*

This section shows the Ulam–Hyers stability of Eq. (18). For simplicity and without loss of generality, we assume $\gamma_1^* = 1$ and $\gamma_2^*, \gamma_3^*, \gamma_4^*$ and $\gamma_5^*$ all are positive. Also we assume $g_1(x_1) = g_2(x_1) = 0$ and $K = 2$. Because finding the exact solution for Eq. (18) is quite difficult, Ulam–Hyers stability guarantees that an approximation of the exact solution could be reached [45]. Let us assume $U^1(t)$ in Eq. (18) has a maximum norm in $C([0,1])$ and for two arbitrary functions $U_1(t)$ and $U_2(t)$ we have

$$\|D^\alpha U_1(t) - D^\alpha U_2(t)\|_{L_{\infty[0,1]}} \le \xi_\alpha\|U_1(t) - U_2(t)\|_{L_{\infty[0,1]}}, \tag{35}$$

where $\xi_\alpha$ is a constant and depends on $\alpha$.

**Theorem 2.** *The fractional differential equation in Eq. (18) is Ulam–Hyers stable.*

**Proof.** To show Eq. (18) is Ulam–Hyers stable, we need to show if $U_m^1(t)$ satisfies the inequality

$$\left|\frac{\partial^\alpha U_m^1(t)}{\partial t^\alpha} + \gamma_2^*\frac{\partial^{\alpha-1}U_m^1(t)}{\partial t^{\alpha-1}} + \gamma_3^* U_m^1(t) + \gamma_4^* D^1 U_m^1(t) + \gamma_5^* D^2 U_m^1(t) - W^1(t)\right| < \varepsilon, \tag{36}$$

then there exists a solution $U^1(t)$ of Eq. (18) satisfying

$$\left|U_m^1(t) - U^1(t)\right| < d\varepsilon, \quad d \in \mathbf{R}.$$

If $U_m^1(t)$ satisfies (36), there exists a function $\phi(t)$ where $|\phi(t)| < \varepsilon$ and

$$\frac{\partial^\alpha U_m^1(t)}{\partial t^\alpha} + \gamma_2^*\frac{\partial^{\alpha-1}U_m^1(t)}{\partial t^{\alpha-1}} + \gamma_3^* U_m^1(t) + \gamma_4^* D^1 U_m^1(t) + \gamma_5^* D^2 U_m^1(t) - W^1(t) = \phi(t), \tag{37}$$

using Eq. (37), we have

$$\left|U_m^1(t) + I^\alpha(\gamma_2^*\frac{\partial^{\alpha-1}U_m^1(t)}{\partial t^{\alpha-1}} + \gamma_3^* U_m^1(t) + \gamma_4^* D^1 U_m^1(t) + \gamma_5^* D^2 U_m^1(t) - W^1(t))\right| = I^\alpha(\phi(t)) \le \frac{\varepsilon}{\Gamma(\alpha+1)}. \tag{38}$$

Suppose $U^1(t)$ is the solution of Eq. (18), using Eq. (38) we have

$$\begin{aligned}
&\|U_m^1(t) - U^1(t)\|_{L_{\infty[0,1]}} \\
&= \|U_m^1(t) + I^\alpha(\gamma_2^* \tfrac{\partial^{\alpha-1}U^1(t)}{\partial t^{\alpha-1}} + \gamma_3^* U^1(t) + \gamma_4^* D^1 U^1(t) + \gamma_5^* D^2 U^1(t) - W^1(t))\|_{L_{\infty[0,1]}} \\
&= ||U_m^1(t) + I^\alpha(\gamma_2^* \tfrac{\partial^{\alpha-1}U^1(t)}{\partial t^{\alpha-1}} + \gamma_3^* U^1(t) + \gamma_4^* D^1 U^1(t) + \gamma_5^* D^2 U^1(t) - W^1(t))+ \\
&\quad I^\alpha(\gamma_2^* \tfrac{\partial^{\alpha-1}U_m^1(t)}{\partial t^{\alpha-1}} + \gamma_3^* U_m^1(t) + \gamma_4^* D^1 U_m^1(t) + \gamma_5^* D^2 U_m^1(t) - W^1(t))- \\
&\quad I^\alpha(\gamma_2^* \tfrac{\partial^{\alpha-1}U_m^1(t)}{\partial t^{\alpha-1}} + \gamma_3^* U_m^1(t) + \gamma_4^* D^1 U_m^1(t) + \gamma_5^* D^2 U_m^1(t) - W^1(t))||_{L_{\infty[0,1]}} \\
&\le \frac{\varepsilon}{\Gamma(\alpha+1)} + \left(\gamma_2^* \xi_{\alpha-1} + \gamma_3^* + \gamma_4^* \xi_1 + \gamma_5^* \xi_2\right)\left(I^\alpha \|U_m^1(t) - U^1(t)\|_{L_{\infty[0,1]}}\right).
\end{aligned} \tag{39}$$

Using Eq. (39) and the Gronwall inequality [41] we have

$$\left|U_m^1(t) - U^1(t)\right| \le \|U_m^1(t) - U^1(t)\|_{L_{\infty[0,1]}} \le \frac{\varepsilon}{\Gamma(\alpha+1)} E_\alpha\left(\left(\gamma_2^* \xi_{\alpha-1} + \gamma_3^* + \gamma_4^* \xi_1 + \gamma_5^* \xi_2\right) t^\alpha\right), \tag{40}$$

where $E_\alpha(t)$ is the Mittag-Leffler function [41]. Using Eq. (40) we have

$$\left|U_m^1(t) - U^1(t)\right| < d\varepsilon$$

where

$$d = \frac{E_\alpha\left(\left(\gamma_2^* \xi_{\alpha-1} + \gamma_3^* + \gamma_4^* \xi_1 + \gamma_5^* \xi_2\right) t^\alpha\right)}{\Gamma(\alpha+1)}$$

so Eq. (18) is Ulam–Hyers stable.

### 4.4. Illustrative example

This section gives examples to demonstrate the applicability and accuracy of the method presented in Section 4.2. We consider Eq. (10) in six different cases; in each case, we compare the method's accuracy with the existing methods reported in the previous papers.

- **Case 1:** In this case, we consider the following FPDE given in [46]

$$\frac{\partial^{0.85} u(x,t)}{\partial t^{0.85}} = \frac{\partial^2 u(x,t)}{\partial x^2} + f(x,t), \tag{41}$$

where

$$f(x,t) = \frac{2}{\Gamma(2.15)}(x^2 - x)t^{1.15} + \pi^2 sin(\pi x) - 2t^2,$$

$$u_{exact}(x,t) = sin(\pi x) + x(x-1)t^2,$$

with the initial and boundary conditions

$$u(x,0) = sin(\pi x), \quad u(0,t) = 0, \quad u(1,t) = 0.$$

This example was studied in [46] using the finite-difference method. Table 1 shows the absolute error for $x = 0.5$ with $M = 5$ and a different value of $K$ using the present method. Fig. 1 shows the approximate and exact solution of Case 1, and Fig. 2 shows the absolute error using the current process. For this example, the best absolute error reported in [46] is $10^{-3}$.

- **Case 2:** In this case, we consider the following FPDE given in [47,48]

$$\frac{\partial^\alpha u(x,t)}{\partial t^\alpha} + \frac{\partial u(x,t)}{\partial x} - \frac{\partial^2 u(x,t)}{\partial x^2} = f(x,t) \tag{42}$$

where

$$f(x,t) = \frac{2t^{2-\alpha}}{\Gamma(3-\alpha)} + (2x - 2),$$

**Table 1**
Absolute error for Case 1.

| t | Present method $K = 2$ | Present method $K = 4$ |
|---|---|---|
| 0.1 | 1.3e−003 | 9.1e−006 |
| 0.2 | 1.5e−003 | 9.4e−006 |
| 0.3 | 1.5e−003 | 8.8e−006 |
| 0.4 | 1.5e−003 | 8.9e−006 |
| 0.5 | 1.5e−003 | 9.2e−006 |
| 0.6 | 1.5e−003 | 9.0e−006 |
| 0.7 | 1.5e−003 | 8.8e−006 |
| 0.8 | 1.6e−003 | 9.4e−006 |
| 0.9 | 1.6e−003 | 9.5e−006 |

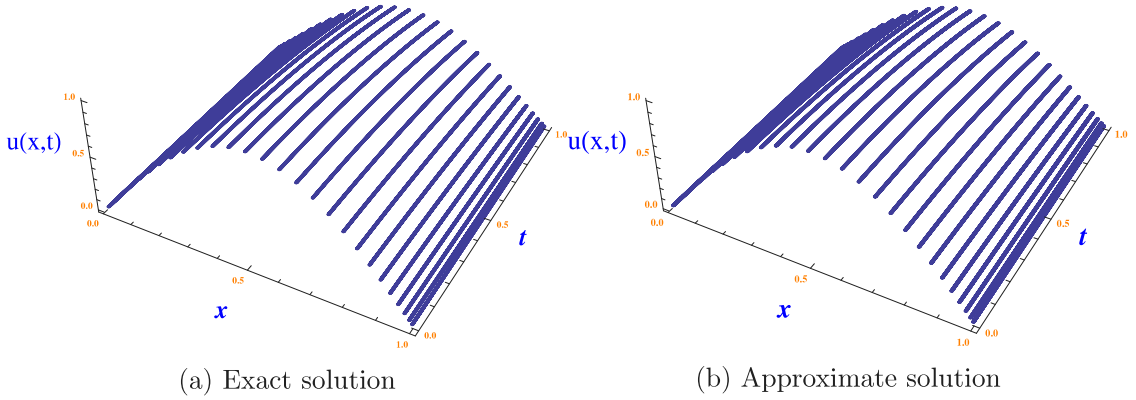


**Fig. 1.** Exact and approximate solution for Case 1.

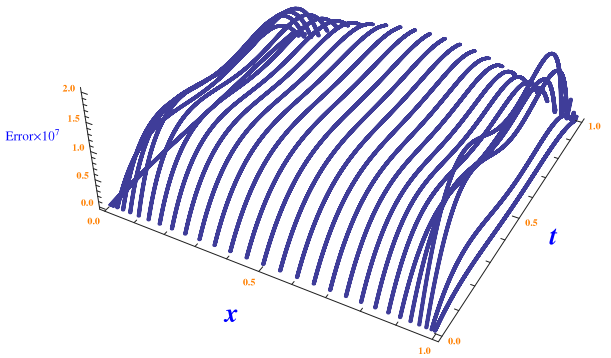


**Fig. 2.** Absolute Error for Case 1.

with the initial and boundary conditions

$$u(x,0) = x^2, \quad u(0,t) = t^2, \quad u(1,t) = 1 + t^2.$$

$$u_{exact}(x,t) = x^2 + t^2.$$

This example was solved in [47] using the Kansa approximation. This example was also considered in [48] by converting it to an NLP problem. The result in [47] is comparable or superior to [48]. Table 2 compares the absolute error obtained for different values of $t$ with $x = 0.5$ and $\alpha = 0.5$ using the present method and method of [47]. Table 3 shows the absolute error for different values of $x$ and $t$. For this example in [47], for different values of $x$ and $t$, the best absolute error is $10^{-5}$.

- **Case 3:** Consider the following time-fractional telegraph equation of order $\alpha$ is given in [26]

$$\frac{\partial^\alpha u(x,t)}{\partial t^\alpha} + \frac{\partial^{\alpha-1} u(x,t)}{\partial t^{\alpha-1}} + u(x,t) - \frac{\partial^2 u(x,t)}{\partial x^2} = f(x,t) \tag{43}$$

**Table 2**
Absolute error for Case 2.

| t | Method of [47] | Present method $M = 1, K = 2$ |
|---|---|---|
| 0.1 | 1.2e−003 | 0.0 |
| 0.5 | 1.0e−003 | 0.0 |
| 1.0 | 6.2e−004 | 0.0 |

**Table 3**
Absolute error for Case 2.

| t | $x = 0.172673$ | $x = 0.5$ | $x = 0.827327$ |
|---|---|---|---|
| 0 | 0 | 0 | 0 |
| 0.1 | 4.1e−017 | 0 | 1.1e−016 |
| 0.2 | 6.9e−017 | 0 | 2.2e−016 |
| 0.3 | 6.9e−017 | 5.5e−017 | 4.4e−016 |
| 0.4 | 1.1e−016 | 0 | 3.3e−016 |
| 0.5 | 1.1e−016 | 0 | 2.2e−016 |
| 0.6 | 1.1e−016 | 0 | 2.2e−016 |
| 0.7 | 1.1e−016 | 0 | 2.2e−016 |
| 0.8 | 1.1e−016 | 0 | 0 |
| 0.9 | 0 | 0 | 0 |

**Table 4**
Absolute error for Case 3.

| $\alpha$ | Present method $M = 4, K = 5$ | Present method $M = 6, K = 5$ |
|---|---|---|
| 1.25 | 1.5e−005 | 5.0e−006 |
| 1.5 | 6.0e−005 | 3.0e−005 |
| 1.75 | 1.4e−004 | 8.0e−005 |
| 1.95 | 8.0e−005 | 5.0e−005 |

where $f(x, t)$ and the boundary and initial conditions are chosen such that the exact solution is

$$u_{exact}(x, t) = x\cos(x^2 + t^2).$$

This example is a fractional telegraph equation considered in [26] using radial basis functions. Table 4 shows the absolute error at $x = 0.5$ for a different value of $\alpha$. In this example, we use piecewise least-squares approximation. For this example in [26], the best absolute error is $10^{-3}$.

- **Case 4:** Consider the partial differential equation [49,50]

$$\frac{\partial^\alpha u(x, t)}{\partial t^\alpha} = \frac{1}{2}x^2\frac{\partial^2 u(x, t)}{\partial x^2} \quad 1 < \alpha \leq 2, \tag{44}$$

the boundary and initial conditions are chosen such that the exact solution is

$$u_{exact}(x, t) = x + x^2\sum_{k=0}^{\infty}\frac{t^{k\alpha+1}}{\Gamma(k\alpha + 2)}.$$

This example is an FPDE studied in [49] and [50] by using Haar wavelets functions and the variational iteration method, respectively. The result in [49] is comparable or superior to [50]; for this example, we compare our results by [49]. In this example, we use piecewise least-squares approximation. In Table 5, we compare the absolute error for a different value of $\alpha$ with [49] that Haar wavelets functions have been used. In this table, $J$ is related to the number of bases used in [49]. The number of bases used in [49] is $2^{2J}$.

**Remark 2.** The numerical method presented in Section 4 solves a wide variety of fractional partial differential equations presented in Eq. (10). Illustrative examples show the validity and applicability of the technique presented in Section 4. The numerical results show the present method's accuracy is comparable or superior to the existing methods reported in the previous papers, such as the Finite-difference method [46], Kansa approximation [47], Radial basis functions [26] and Haar wavelets functions [49]. The comparison details are presented in each example, and Table 6 summarizes this comparison. Also, the numerical results show the present method is less time-consuming than the existing methods reported in the previous papers because it needs less number of bases to provide less error. The numerical method presented in Section 4 can be used for solving fractional partial differential equations that have the fractional order derivative in time and the integer order derivative in space, and this method cannot solve fractional partial differential equations with the fractional derivative in space. This point is a limitation of the present scenario. Also, the current method approximates the solution

**Table 5**
Absolute error for Case 4.

| Method | Absolute error |
|---|---|
| Method of [49] | |
| $\alpha = 1.5, \quad t = 0.2, \quad J = 6$ | $2.3 \times 10^{-5}$ |
| $\alpha = 1.5, \quad t = 0.2, \quad J = 7$ | $2.4 \times 10^{-6}$ |
| $\alpha = 1.75, \quad t = 0.2, \quad J = 6$ | $6.1 \times 10^{-6}$ |
| $\alpha = 1.75, \quad t = 0.2, \quad J = 7$ | $1.7 \times 10^{-6}$ |
| Present Method | |
| $\alpha = 1.5, \quad t = 0.2, \quad M = 5, \ K = 8$ | $6.1 \times 10^{-9}$ |
| $\alpha = 1.5, \quad t = 0.2, \quad M = 6, \ K = 8$ | $2.8 \times 10^{-9}$ |
| $\alpha = 1.75, \quad t = 0.2, \quad M = 5, \ K = 8$ | $1.4 \times 10^{-9}$ |
| $\alpha = 1.75, \quad t = 0.2, \quad M = 6, \ K = 8$ | $6.3 \times 10^{-10}$ |

**Table 6**
Comparing the present method's accuracy with the existing methods reported in the previous papers.

| Example | Absolute error | Absolute error |
|---|---|---|
| Case 1 | Present method $10^{-6}$ | Finite-difference method [46] $10^{-3}$ |
| Case 2 | Present method 0 | Kansa approximation [47] $10^{-5}$ |
| Case 3 | Present method $10^{-5}$ | Radial basis functions [26] $10^{-3}$ |
| Case 4 | Present method $10^{-9}$ | Haar wavelets functions [49] $10^{-6}$ |

at the discretization points. In the next section, we use the numerical method presented in Section 4.2 to evaluate the fractional forward Kolmogorov equations in population genetics.

## 5. Fractional forward Kolmogorov equations in population genetics

The coalescent theory describes the evolution of a population backward in time. Because of heterogeneity, different productivities in the population's environments will lead to fluctuating offspring variability. Using the coalescent theory, the author recently show that heterogeneity affects the time to the most recent common ancestor [15]. This result shows that the order of fractional derivative, $\alpha$, of the fractional coalescence measures these fluctuations where $\alpha = 1$ leads to no fluctuations and small $\alpha$ marks large fluctuations. While in the backward process, using the coalescent theory, we calculated the time to the most recent ancestor, using the diffusion theorem in the forward process, we will be able to calculate the time of fixation. Since several successive generations will have the same most recent common ancestor and the genes destined for fixation in several successive generations may attain fixation in the same generation, there is no natural correspondence between coalescent and fixation events. However, for the case where the dynamics of gene frequencies are Markovian, i.e., depending on the present but not previous frequencies, the average coalescent time and average fixation time for the entire population are equal [38–40]. Based on these results, the order of fractional derivative in Eq. (9) is a candidate that shows the effect of heterogeneity. This is the first interpretation of the order of fractional derivatives in population genetics.

To study the effect of heterogeneity on DAF, we use the numerical method developed in Section 4.2 to solve the fractional forward Kolmogorov equations in population genetics in Eq. (9). For the Wright–Fisher model, $b(x) = x(1-x)$ and $a(x)$ has different forms depending on the evolutionary forces. We considered pure drift and mutation as evolutionary forces to study the solution of fractional forward Kolmogorov Eq. (9). Because the numerical method presented in Section 4.2 provides the solution of FPDEs at Legendre–Gauss–Lobatto collocation points, we study the DAF at these points by considering pure drift and mutation as evolutionary forces. Since the initial condition is unknown, we choose different functions for the initial condition.

### 5.1. Pure drift

Under pure drift, for the Wright–Fisher model $a(x) = 0$ and $b(x) = x(1-x)$. To use the numerical method presented in Section 4.2, we use the piecewise least-squares approximation by choosing three subintervals while we use $K = 4$ and $M = 3$. Fig. 3 shows the DAF at the first discretization point under pure drift. This Figure shows that under pure drift, the initial condition changes DAF's behavior by considering heterogeneity's impact. For the $u(x, 0) = 1$ and $u(x, 0) = e^x$ as initial conditions, DAF decreases rapidly by decreasing the effect of heterogeneity. Also, this Figure shows that for the $u(x, 0) = x$ and $u(x, 0) = sinx$ as initial conditions, DAF increases rapidly by decreasing the effect of heterogeneity.

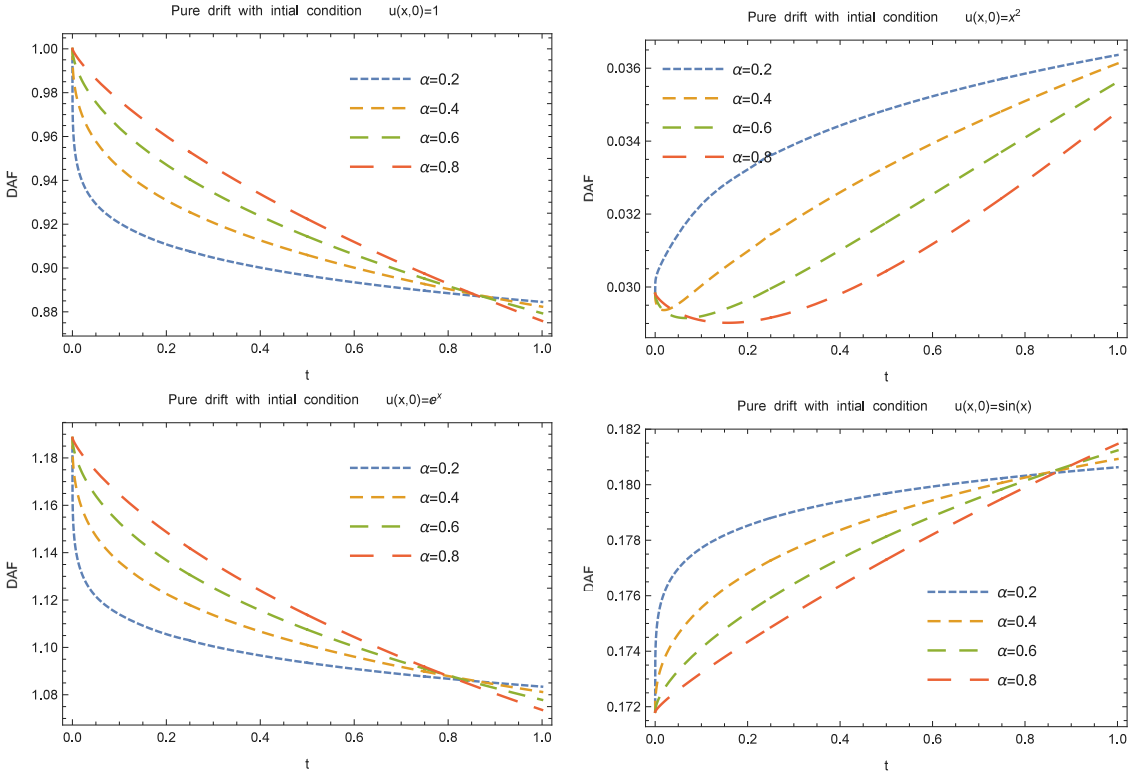


**Fig. 3.** Allele frequency distribution (DAF) by considering pure drift as evolutionary force.

### 5.2. Mutation

We assume the Wright–Fisher model and a biallelic locus. Under mutation, $a(x) = -\mu x + \nu(1-x)$ where $\mu$ and $\nu$ be the scaled mutations rates and $b(x) = x(1-x)$. To use the numerical method presented in Section 4.2, we use the piecewise least-squares approximation by choosing three subintervals while we use $K = 4$ and $M = 3$. Figs. 4, 5, and 6 show the DAF at the first discretization point under mutation. Figs. 4, 5, and 6 show the DAF under different mutation rates, the same mutation rate less than 0.5 and the same mutation rate greater than 0.5, respectively. Fig. 4 shows under different mutation rates; the initial condition does not change the behavior of DAF by considering the impact of heterogeneity. Also, this Figure shows, under different mutation rates, DAF increases rapidly by decreasing the effect of heterogeneity. Fig. 5 shows that under the same mutation rate of less than 0.5, the initial condition changes DAF's behavior by considering heterogeneity's impact. This Figure shows that for the $u(x, 0) = 1$ and $u(x, 0) = e^x$ as initial conditions, DAF decreases rapidly by decreasing the effect of heterogeneity. Also, this Figure shows that for the $u(x, 0) = x$ and $u(x, 0) = sinx$ as initial conditions, DAF increases rapidly by decreasing the effect of heterogeneity. Fig. 6 shows under the same mutation rate greater than 0.5; the initial condition does not change the behavior of DAF by considering the impact of heterogeneity. Also, this Figure shows that under the same mutation rate greater than 0.5, DAF decreases more slowly by increasing the effect of heterogeneity.

## 6. Conclusion

This paper introduces the fractional forward Kolmogorov equations in population genetics. We developed the theory base on the assumption that the order of fractional derivatives shows the effect of heterogeneity in the population. The distribution of allele frequencies is the solution of fractional forward Kolmogorov equations. To derive the distribution of allele frequencies, we developed the numerical method for solving the general form of the fractional partial differential equations. Using the new numerical method, we study the effect of heterogeneity on the distribution of allele frequencies.

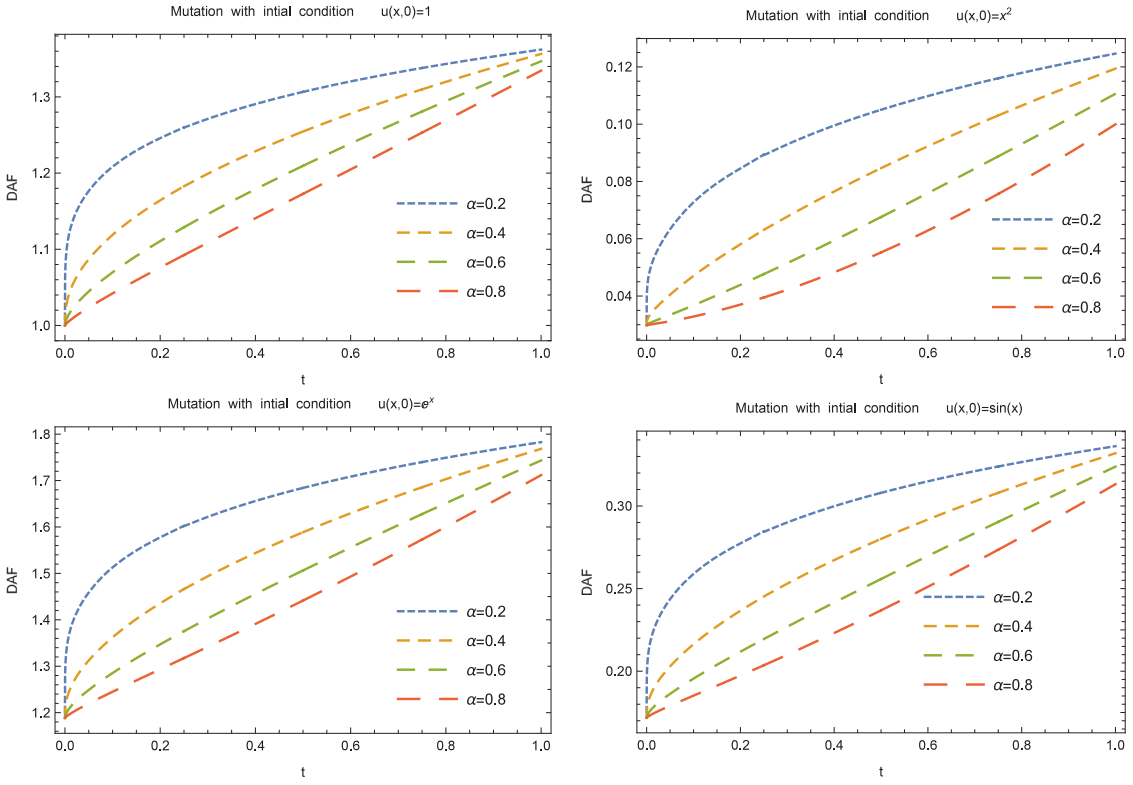


**Fig. 4.** Allele frequency distribution (DAF) by considering mutation as the evolutionary force with the different mutation rates.

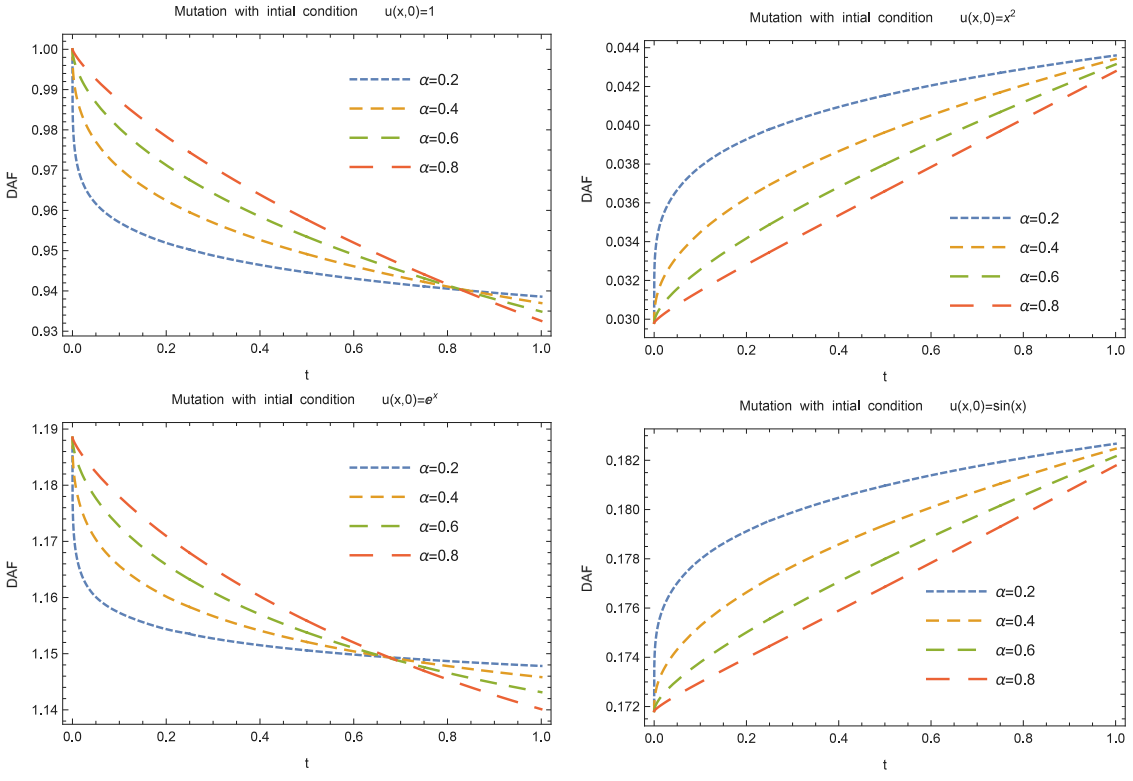


**Fig. 5.** Allele frequency distribution (DAF) by considering mutation as the evolutionary force with the same mutation rate less than 0.5.

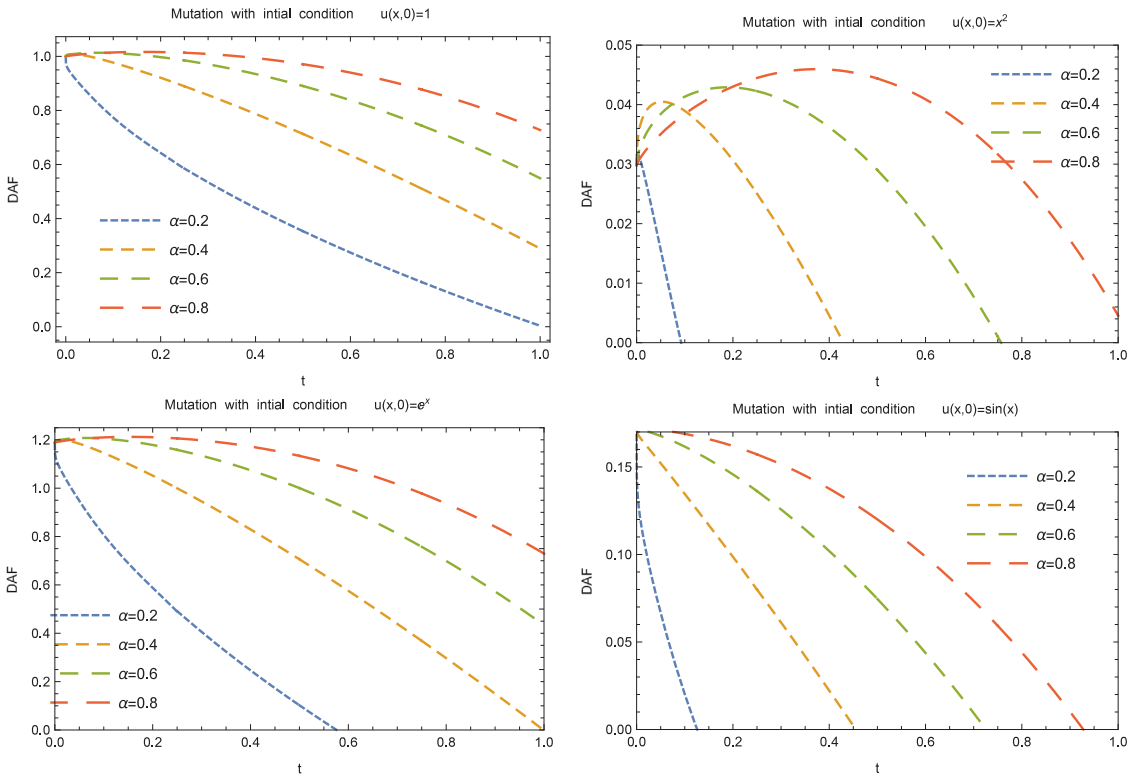


**Fig. 6.** Allele frequency distribution (DAF) by considering mutation as the evolutionary force with the same mutation rate greater than 0.5.

## Declaration of competing interest

There are no known conflicts of interest associated with this publication, and there has been no significant financial support for this work that could have influenced its outcome.

## Data availability

No data was used for the research described in the article.

## Acknowledgments

The National Science Foundation, United States supported Somayeh Mashayekhi's grant DBI 2109990.

## References

[1] Tataru Paula, Simonsen Maria, Bataillon Thomas, Hobolth Asger. Statistical inference in the wright–Fisher model using allele frequency data. Syst Biol 2017;66(1):e30–46.
[2] Wakeley John. The limits of theoretical population genetics. Genetics 2005;169(1):1–7.
[3] Fisher Ronald Aylmer. The genetical theory of natural selection. 1958.
[4] Wright Sewall. Evolution in mendelian populations. Genetics 1931;16(2):97.
[5] Kingman John FC, Koch G, Spizzichino F. Exchangeability and the evolution of large populations. Exchangeability Probab Stat 1982;91:112.
[6] Kingman John FC. On the genealogy of large populations. J Appl Probab 1982;19(A):27–43.
[7] Kingman John Frank Charles. The coalescent. Stoch Process Appl 1982;13(3):235–48.
[8] Kingman John FC. Origins of the coalescent: 1974–1982. Genetics 2000;156(4):1461–3.
[9] Wright Sewall. The differential equation of the distribution of gene frequencies. Proc Natl Acad Sci 1945;31(12):382–9.
[10] Kimura Motoo. Some problems of stochastic processes in genetics. Ann Math Stat 1957;882–901.
[11] Cavalli-Sforza Luigi L, Edwards Anthony WF. Phylogenetic analysis. Models and estimation procedures. Am J Hum Genet 1967;19(3 Pt 1):233.
[12] Noorbakhsh Javad, Kim Hyunsoo, Namburi Sandeep, Chuang Jeffrey H. Distribution-based measures of tumor heterogeneity are sensitive to mutation calling and lack strong clinical predictive power. Sci Rep 2018;8(1):1–12.
[13] Ramón y Cajal Santiago, Sesé Marta, Capdevila Claudia, Aasen Trond, Mattos-Arruda De, Diaz-Cano Salvador J, et al. Clinical implications of intratumor heterogeneity: challenges and opportunities. J Mol Med 2020;98(2):161–77.
[14] Liu Jinping, Dang Hien, Wang Xin Wei. The significance of intertumor and intratumor heterogeneity in liver cancer. Exp Mol Med 2018;50(1):e416.

[15] Mashayekhi Somayeh, Beerli Peter. Fractional coalescent. Proc Natl Acad Sci 2019;116(13):6244–9.
[16] Mashayekhi Somayeh, Miles Paul, Hussaini M Yousuff, Oates William S. Fractional viscoelasticity in fractal and non-fractal media: Theory, experimental validation, and uncertainty analysis. J Mech Phys Solids 2018;111:134–56.
[17] Mashayekhi Somayeh, Hussaini M Yousuff, Oates William. A physical interpretation of fractional viscoelasticity based on the fractal structure of media: theory and experimental validation. J Mech Phys Solids 2019;128:137–50.
[18] Mashayekhi Somayeh, Stanisauskis Eugenia, Hassani Mahdi, Oates William. Excluded volume effects and fractional viscoelasticity in polymers. Meccanica 2022;57(4):821–32.
[19] Stanisauskis Eugenia, Mashayekhi Somayeh, Pahari Basanta, Mehnert Markus, Steinmann Paul, Oates William. Fractional and fractal order effects in soft elastomers: Strain rate and temperature dependent nonlinear mechanics. Mech Mater 2022;172:104390.
[20] Magin Richard L. Fractional calculus in bioengineering. Vol. 2, Begell House Redding; 2006.
[21] Magin Richard L. Fractional calculus models of complex dynamics in biological tissues. Comput Math Appl 2010;59(5):1586–93.
[22] Ezz-Eldien SS. On solving fractional logistic population models with applications. Comput Appl Math 2018;37(5):6392–409.
[23] Abadias Luciano, Estrada-Rodriguez Gissell, Estrada Ernesto. Fractional-order susceptible-infected model: Definition and applications to the study of COVID-19 main protease. Fract Calc Appl Anal 2020;23:635–55.
[24] Jumarie Guy. Modified Riemann-Liouville derivative and fractional Taylor series of nondifferentiable functions further results. Comput Math Appl 2006;51(9–10):1367–76.
[25] Wu Jiunn-Lin. A wavelet operational method for solving fractional partial differential equations numerically. Appl Math Comput 2009;214(1):31–40.
[26] Hosseini Vahid Reza, Chen Wen, Avazzadeh Zakieh. Numerical solution of fractional telegraph equation by using radial basis functions. Eng Anal Bound Elem 2014;38:31–9.
[27] Podlubny Igor. The Laplace transform method for linear differential equations of the fractional order. 1997, arXiv preprint funct-an/9710005.
[28] Odibat Zaid, Momani Shaher. A generalized differential transform method for linear partial differential equations of fractional order. Appl Math Lett 2008;21(2):194–9.
[29] Orsingher Enzo, Zhao Xuelei. The space-fractional telegraph equation and the related fractional telegraph process. Chin Ann Math 2003;24(01):45–56.
[30] Momani Shaher. Analytic and approximate solutions of the space-and time-fractional telegraph equations. Appl Math Comput 2005;170(2):1126–34.
[31] Yıldırım Ahmet. He's homotopy perturbation method for solving the space-and time-fractional telegraph equations. Int J Comput Math 2010;87(13):2998–3006.
[32] Das Subir, Vishal K, Gupta PK, Yildirim A. An approximate analytical solution of time-fractional telegraph equation. Appl Math Comput 2011;217(18):7405–11.
[33] Chen Wen, Ye Linjuan, Sun Hongguang. Fractional diffusion equations by the Kansa method. Comput Math Appl 2010;59(5):1614–20.
[34] Podlubny Igore. Fractional differential equations. Math Sci Eng 1999;198:41–119.
[35] Osler Thomas J. Taylor's series generalized for fractional derivatives and applications. SIAM J Math Anal 1971;2(1):37–48.
[36] Odibat Zaid M, Shawagfeh Nabil T. Generalized Taylor's formula. Appl Math Comput 2007;186(1):286–93.
[37] Chandra Suresh, Sharma Mohair Kumar. A textbook of statistical mechanics. CBS Publishers & Distributors Pvt Ltd, India; 2016.
[38] Campbell RB. The coalescent time in the presence of background fertility selection. Theor Popul Biol 1999;55(3):260–9.
[39] Campbell RB. Coalescent size versus coalescent time with strong selection. Bull Math Biol 2007;69(7):2249–59.
[40] Greenbaum Gili. Revisiting the time until fixation of a neutral mutant in a finite population–a coalescent theory approach. J Theoret Biol 2015;380:98–102.
[41] Mashayekhi S, Sedaghat S. Fractional model of stem cell population dynamics. Chaos Solitons Fractals 2021;146:110919.
[42] Mashayekhi Somayeh, Ixaru L Gr. The least-squares fit of highly oscillatory functions using Eta-based functions. J Comput Appl Math 2020;376:112839.
[43] Burden RL, Faires J Douglas, Reynolds A. Numerical analysis, brooks/cole. Boston, Mass, USA; 2010.
[44] Canuto Claudio, Hussaini M Yousuff, Quarteroni Alfio, Zang Thomas A. Spectral methods: fundamentals in single domains. Springer Science & Business Media; 2007.
[45] Ahmed E, El-Sayed AMA, El-Saka HAA, Ashry Gehan A. On applications of Ulam-Hyers stability in biology and economics. 2010, arXiv preprint arXiv:1004.1354.
[46] Xu Yufeng, He Zhimin, Agrawal Om P. Numerical and analytical solutions of new generalized fractional diffusion equation. Comput Math Appl 2013;66(10):2019–29.
[47] Uddin Marjan, Haq Sirajul. RBFs approximation method for time fractional partial differential equations. Commun Nonlinear Sci Numer Simul 2011;16(11):4208–14.
[48] Ghandehari Mohammad Ali Mohebbi, Ranjbar Mojtaba. A numerical method for solving a fractional partial differential equation through converting it into an NLP problem. Comput Math Appl 2013;65(7):975–82.
[49] ur Rehman Mujeeb, Khan Rahmat Ali. Numerical solutions to initial and boundary value problems for linear fractional partial differential equations. Appl Math Model 2013;37(7):5233–44.
[50] Momani Shaher, Odibat Zaid. Analytical approach to linear fractional partial differential equations arising in fluid mechanics. Phys Lett A 2006;355(4–5):271–9.